UKnowledge

University of Kentucky
UKnowledge

Chemistry Faculty Publications   Chemistry

5-16-2018

Spectroscopy and Formation of Lanthanum-Hydrocarbon Radicals Formed by Association and Carbon-Carbon Bond Cleavage of Isoprene

Wenjin Cao
University of Kentucky, wj.cao0707@uky.edu

Dilkrushi Hewage
University of Kentucky, dche223@uky.edu

Dong-Sheng Yang
University of Kentucky, Dong-Sheng.Yang@uky.edu

Right click to open a feedback form in a new tab to let us know how this document benefits you.

Follow this and additional works at: https://uknowledge.uky.edu/chemistry_facpub

🎨 Part of the Biological and Chemical Physics Commons, Chemistry Commons, and the Plasma and Beam Physics Commons

Spectroscopy and Formation of Lanthanum-Hydrocarbon Radicals Formed by Association and Carbon-Carbon Bond Cleavage of Isoprene

Spectroscopy and formation of lanthanum-hydrocarbon radicals formed by association and carbon-carbon bond cleavage of isoprene

Wenjin Cao, Dilrukshi Hewage, and Dong-Sheng Yang

Articles you may be interested in

Spectroscopy and formation of lanthanum-hydrocarbon radicals formed by C—H and C—C bond activation of 1-pentene and 2-pentene
The Journal of Chemical Physics **149**, 034303 (2018); 10.1063/1.5022771

Photofragment imaging and electronic spectroscopy of Al_2^+
The Journal of Chemical Physics **148**, 214308 (2018); 10.1063/1.5034353

Dissociation dynamics of 3- and 4-nitrotoluene radical cations: Coherently driven $C–NO_2$ bond homolysis
The Journal of Chemical Physics **148**, 134305 (2018); 10.1063/1.5024892

Time-resolved photoelectron spectroscopy of adenosine and adenosine monophosphate photodeactivation dynamics in water microjets
The Journal of Chemical Physics **148**, 194303 (2018); 10.1063/1.5027258

Spectroscopy and formation of lanthanum-hydrocarbon radicals formed by C—C bond cleavage and coupling of propene
The Journal of Chemical Physics **146**, 184304 (2017); 10.1063/1.4982949

Lanthanum-mediated dehydrogenation of 1- and 2-butynes: Spectroscopy and formation of $La(C_4H_4)$ isomers
The Journal of Chemical Physics **147**, 064303 (2017); 10.1063/1.4997567

Spectroscopy and formation of lanthanum-hydrocarbon radicals formed by association and carbon-carbon bond cleavage of isoprene

Wenjin Cao, Dilrukshi Hewage, and Dong-Sheng Yang[a)]
Department of Chemistry, University of Kentucky, Lexington, Kentucky 40506-0055, USA

La atom reaction with isoprene is carried out in a laser-vaporization molecular beam source. The reaction yields an adduct as the major product and C—C cleaved and dehydrogenated species as the minor ones. $La(C_5H_8)$, $La(C_2H_2)$, and $La(C_3H_4)$ are characterized with mass-analyzed threshold ionization (MATI) spectroscopy and quantum chemical computations. The MATI spectra of all three species exhibit a strong origin band and several weak vibronic bands corresponding to La-ligand stretch and ligand-based bend excitations. $La(C_5H_8)$ is a five-membered metallacycle, whereas $La(C_2H_2)$ and $La(C_3H_4)$ are three-membered rings. All three metallacycles prefer a doublet ground state with a La $6s^1$-based valence electron configuration and a singlet ion. The five-membered metallacycle is formed through La addition and isoprene isomerization, whereas the two three-membered rings are produced by La addition and insertion, hydrogen migration, and carbon-carbon bond cleavage. *Published by AIP Publishing.* https://doi.org/10.1063/1.5026899

I. INTRODUCTION

Hydrocarbon compounds are ubiquitous in nature and the most abundant, low-cost feedstock for functionalized organic chemicals yet many of which are too inert to participate in chemical reactions under mild conditions. Metal activation helps us to mitigate this problem by stimulating inert hydrocarbons to react with other molecules. To better understand how metal centers activate C—H/C bonds, spectroscopy of transition metal-hydrocarbon species formed in gas phase reactions has recently attracted considerable attention. Metal ion-hydrocarbon species are largely investigated by infrared or ultraviolet-visible photodissociation or photoelectron spectroscopy,[1–34] whereas metal atom-hydrocarbon radicals are mainly studied by resonant two-photon ionization and dispersed fluorescence,[35–38] Fourier transform microwave,[39] and mass analyzed threshold ionization (MATI) spectroscopy.[40–48] Spectroscopic measurements probe state specific energies and structures of short-lived species, which are vital for gaining insight into reaction mechanisms and electronic and structural characteristics for efficient bond activation at metal centers. Such measurements can also be used to test electronic structure calculations, where computations are complicated by possibly multiple low-energy isomers of each metal-containing species and high-density of low-lying electronic states or spin-orbit levels of each isomer. On the other hand, spectroscopic measurements of transition metal-hydrocarbon species formed by the C—H or C—C bond activation of hydrocarbon compounds encounter substantial challenges because such species are produced with a low number density and often in an open-shell electronic state. We have recently reported the MATI spectroscopy and formation of the metal-hydrocarbon

radicals produced by the lanthanide-mediated C—C or C—H bond activation of several small alkenes and alkynes.[40–48] Our studies demonstrate that the combination of the MATI spectroscopic measurements with electronic structure calculations is a powerful approach to investigate transient metal-hydrocarbon species.

Isoprene (2-methyl-1,3-butadiene) is one of the most abundant volatile organic compounds in the troposphere. Its emission affects the aerosol formation and contributes to the formation of tropospheric ozone in the presence of nitric oxides.[40] Its industrial applications are largely for polydiene production. The most effective method for the precise control of polydienes is coordination-insertion polymerization accomplished by single-site transition metal catalysts.[49] Although isoprene reactions with metal ions or atoms in the gas phase have rarely been reported, metal ion reactions with its parent molecule, 1,3-butadiene, have been investigated with mass spectrometry based methods. Bohme and co-workers observed sequential additions of the butadiene to Fe^+ (up to four ligands) using a selected-ion flow tube technique.[50] Freiser and co-workers detected M^+(1,3-butadiene) adduct as the only product for M = Ni but both M^+(1,3-butadiene) and $M^+(C_4H_4)$ corresponding to a H_2 loss for M = Fe and Co using Fourier transform ion cyclotron resonance (FTICR) mass spectrometry.[51] In contrast to the late transition metal ions, Ohanessian and co-workers observed, also with FTICR, $W^+(C_4H_4)$ as the major product, with minor amounts of $W^+(C_2H_2)$ and of $W^+(C_3H_2)$.[52] In reactions with transition metal oxide ions, Castleman and co-workers observed using a triple quadruple mass spectrometer system that tantalum oxide cluster ions cleaved the butadiene to give $Ta_xO_y^+(C_2H_4)$ as the major reaction,[53,54] whereas vanadium oxide cluster ion reactions yielded $V_xO_y^+(C_4H_6)$ as the major products, with minor amounts of $V_xO_y^+(C_4H_4)$ and $V_xO_y^+(C_2H_3)$.[55] 1,3-butadiene reactions with neutral vanadium oxide clusters have been studied

[a)]Author to whom correspondence should be addressed: dyang0@uky.edu

by Bernstein, He, and co-workers, where $V_xO_y(C_3H_4)$ and $V_xO_y(C_4H_6)$ were detected through soft x-ray photoionization.[56] In all of the aforementioned studies, no spectroscopic measurements were reported.

In a very recent study, we reported spectroscopic characterization of nonconcerted [4 + 2] cycloaddition of 1,3-butadiene with lanthanacyclopropene [La(CH═CH)] to form La(benzene).[44] Lanthanacyclopropene is an intermediate generated by the primary reaction between La and 1,3-butadiene, and computational prediction suggests that the formation of this intermediate involves La addition, 1,3-butadiene isomerization, 1,3 or 4,2-H migration, and C2─C3 bond cracking. To test the computational prediction, we carried out a MATI spectroscopic study of the metal radicals formed by the La + isoprene reaction. Because the H atom on the C2 position of 1,3-butadiene is replaced by a methyl group in isoprene, a 1,3-H migration followed by the cleavage of the isoprene C2─C3 single bond is expected to form a methyl-substitute lanthana-cyclopropene [La(CH═CCH₃)] + ethylene, whereas a 4,2-H migration followed by the C2─C3 bond cracking should produce lanthanacyclopropene [La(CH═CH)] + propene. Competing with the 1,3-H migration, a H atom in the methyl group could also migrate to C3 to form La[H₂CC(CH₂)CH₂CH₂] which then may decompose to La(CH₂═C═CH₂) + ethylene or La(CH₂CH₂) + allene through the cleavage of the C2─C3 single bond. We report here the MATI spectroscopy and formation of La-hydrocarbon radicals formed by molecular addition and C─C bond cleavage. In this work, we observe both La(CH═CH) and La(CH═CCH₃), confirming the previously proposed pathway for the formation of La(CH═CH) from the La + 1,3-butadiene reaction. On the other hand, we detect no traces of La[H₂CC(CH₂)CH₂CH₂], La(CH₂═C═CH₂), or La(CH₂CH₂), suggesting that a H migration from the methyl group of isoprene is insignificant in the La + isoprene reaction.

II. EXPERIMENTAL AND COMPUTATIONAL METHODS

A. Experimental

The metal-cluster beam instrument used in this work consists of reaction and spectroscopy vacuum chambers and was described in a previous publication.[57] The La-isoprene reaction was carried out in a laser-ablation metal cluster beam source. La atoms were generated by pulsed laser (Nd:YAG, Continuum Minilite II, 532 nm, ~1.0 mJ/pulse) ablation of a La rod (99.9%, Alfa Aesar) in the presence of a He (99.998%, Scott Gross) carrier gas (40 psi) delivered by a home-made piezoelectric pulsed valve. Vapor of isoprene (boiling point 34 °C, 99%, Aldrich) was introduced 3 cm downstream of the laser ablation point, from which La atoms, He gas, and the isoprene vapor entered into a collision tube (2 mm diameter and 2 cm length) and were then expanded into the reaction chamber, collimated by a cone-shaped skimmer (2 mm inner diameter), and passed through a pair of deflection plates. Ionic species in the molecular beam that were formed by laser ablation were removed by an electric field (100 V cm⁻¹) applied on the deflection plates, and neutral products were identified by photoionization time-of-flight (TOF) mass spectrometry.

Prior to the MATI measurements, photoionization efficiency spectra of La-hydrocarbon radicals were recorded to locate an approximate ionization threshold to guide MATI scans. In the MATI experiment, the La-hydrocarbon radicals were excited to high-lying Rydberg states in a single-photon process and ionized by a delayed pulsed electric field. The excitation laser was the frequency doubled output of a tunable dye laser (Lumonics HD-500), pumped by the third harmonic output (355 nm) of a Nd:YAG laser (Continuum Surelite II). The laser beam was collinear and counter-propagating with the molecular beam. The ionization pulsed field (320 V cm⁻¹), which was also used for accelerating ions into the field free region, was generated by two high voltage pulse generators (DEI, PVX-4140) and delayed by ~20 μs from the laser pulse by a delayed pulsed generator (SRS, DG645). A small dc field (6.0 V cm⁻¹) from another power supply (GW INSTEK, GPS-30300) was used to separate the ions produced by direct photoionization from the MATI ions generated by the delayed field ionization. The MATI ion signals were obtained by scanning the tunable dye laser, detected by a dual microchannel plate detector, amplified by a preamplifier (SRS, SR445), visualized by a digital oscilloscope (Tektronix TDS 3012), and stored in a laboratory computer. Laser wavelengths were calibrated against titanium atomic transitions in the MATI spectral region, and the calibration was done after recording the MATI spectra.[58] The Stark shift on the adiabatic ionization energy (ΔAIE) induced by the dc field (E_f) was calculated using the relation of $\Delta AIE = 6.1E_f^{1/2}$, where E_f is in V cm⁻¹ and ΔAIE is in cm⁻¹.[59]

B. Computational

The density functional theory (DFT) method with Becke's three-parameter hybrid functional with the correlation functional of Lee, Yang, and Parr (B3LYP) was used to calculate the equilibrium geometries and vibrational frequencies of the La-hydrocarbon radicals and single charged positive ions. The basis sets used in these calculations were 6-311+G(d,p) for C and H and the Stuttgart/Dresden (SDD) effective-core-potential basis set with 28-electron core for La. We have extensively used the DFT/B3LYP method and found that this method generally produced adequate results for spectral and structural assignments of organometallic radicals.[40–42,44–48,60] No symmetry restrictions were imposed in initial geometry optimizations, but appropriate point groups were used in subsequent optimizations to help identify electronic symmetries. For each optimized stationary point, a vibrational analysis was performed to identify the nature of the stationary point (minimum or saddle point). In predicting reaction pathways, minima connected by a transition state were confirmed by intrinsic reaction coordinate calculations. To refine the energies of the electronic states, single-point energy calculations were carried out with the coupled cluster with single, double, and perturbative triple excitations [CCSD(T)] method. These calculations involve the third-order Douglas-Kroll-Hess scalar relativistic correction and are at the DFT/B3LYP optimized geometries. Basis sets used in the CCSD(T) calculations were cc-pVTZ-DK[61,62] for C and H and cc-pVTZ-DK3[63] for La. The DFT calculations were performed with the Gaussian 09
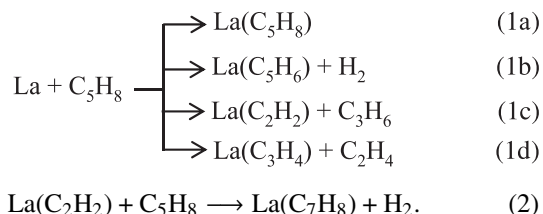
software package,[64] whereas the CCSD(T) calculations were carried out with MOLPRO 2010.1.[65]

To compare with the experimental MATI spectra, multi-dimensional Franck-Condon (FC) factors were calculated from the equilibrium geometries, harmonic vibrational frequencies, and normal coordinates of the neutral and ionized complexes.[66] In these calculations, the recursion relations from Doktorov *et al.*[67] were employed, and the Duschinsky effect[68] was considered to account for a possible axis rotation from the neutral complex to the cation. Spectral simulations were obtained using the experimental linewidth and Lorentzian line shape. Transitions from excited vibrational levels of the neutral complex were considered by assuming thermal excitation at specific temperatures.

III. RESULTS AND DISCUSSION

A. TOF mass spectrum and La-hydrocarbon species

Figure 1 displays the TOF mass spectra of the La + isoprene reaction recorded with 235 nm photoionization. The spectra show La-hydrocarbon species corresponding La(C_nH_m) (n = 2, 3, 5, and 7; m = 2, 4, 6, and 8). These species may be formed through following primary and secondary reactions:

$$La + C_5H_8 \longrightarrow \begin{cases} La(C_5H_8) & (1a) \\ La(C_5H_6) + H_2 & (1b) \\ La(C_2H_2) + C_3H_6 & (1c) \\ La(C_3H_4) + C_2H_4 & (1d) \end{cases}$$

$$La(C_2H_2) + C_5H_8 \longrightarrow La(C_7H_8) + H_2. \quad (2)$$

The primary reactions (1a)–(1d) include molecular association, dehydrogenation, and C—C bond cleavage, whereas the secondary reaction (2) involves addition of a second isoprene molecule to one of the C—C bond cleaved species La(C_2H_2) followed by a loss of H_2. Although the reaction channels are similar to those observed for the La + 1,3-butadiene reaction,[44] branching ratios (BRs) of the metal-hydrocarbon species formed in these channels are considerably different. In the isoprene reaction, the adduct La(C_5H_8) is by far the most predominant (BR = 0.65), all other species from the primary reactions are relatively minor, and the only species from the secondary reaction is even less. By contrast, the La + 1,3-butadiene reactions yields La(C_2H_2) from the C—C bond cleavage as the major product (BR = 0.44) and other species from association, dehydrogenation, or secondary reactions as the minor ones. These observations suggest that the methyl substitution of a hydrogen atom in the C2 position of 1,3-butadiene decreases the hydrocarbon reactivity toward the La atom, especially the reaction channel of the C—C bond cleavage. In addition to the metal-hydrocarbon species, a significant amount of LaO is observed. LaO could be formed by La reactions with oxygen that is present in the carrier gas as an impurity or by laser vaporization of La oxide impurity in the La rod.[40–42,44–48] In the following paragraphs, we will focus on the spectroscopic and computational characterization of La(C_5H_8) formed through association and La(C_2H_2) and La(C_3H_4) formed through C—C bond cracking.

B. La(C_5H_8)

The MATI spectrum of La(C_5H_8) formed by the La + isoprene reaction [Fig. 2(a)] shows the strongest band at 39 007 (5) cm^{-1}, 352 and 427 cm^{-1} progression with up to two vibrational quanta, and several weak bands (100, 235, 295, 474, and 502 cm^{-1}) at the higher energy side of the strongest band, and two additional weak bands (110 and 342 cm^{-1}) at the lower energy side. Transitions marked with "*1-*3" are combination bands of 352 cm^{-1} with 235, 295, and 427 cm^{-1}, respectively. The strongest band is easily assigned as the origin band, and its energy corresponds to the AIE of the metal-hydrocarbon radical. The strong origin band coupled with the short spectral profile indicates that the geometries of the neutral species and singly charged cation are similar, whereas the observation of numerous bands suggests that the metal-hydrocarbon radical must have a low molecular symmetry.

Two possible isomers of La(C_5H_8), Iso A (C_1) and Iso B (C_1), are shown in Figs. 3(a) and 3(b), and their relative energies are listed in Table I. Iso B is a three-membered lanthanacycle with La binding with C2 and C3 atoms of the *trans*-isoprene. In the free *trans*-isoprene, the two C=C bonds are predicted by DFT/B3LYP to be 1.338 and 1.342 Å and the C2—C3 single bond is predicted to be 1.467 Å. Upon La addition, the two double bonds are extended to 1.439 and 1.437Å, whereas the single bond is reduced to 1.410 Å so that the three CC bonds become comparable. This metal-mediated perturbation on the hydrocarbon structure can be understood from interactions between the frontier orbitals of the diene molecule and 5d orbitals of the La atom. In a butadiene molecule, the four C pπ orbitals of the highest occupied molecular orbital (HOMO) are in a bonding configuration
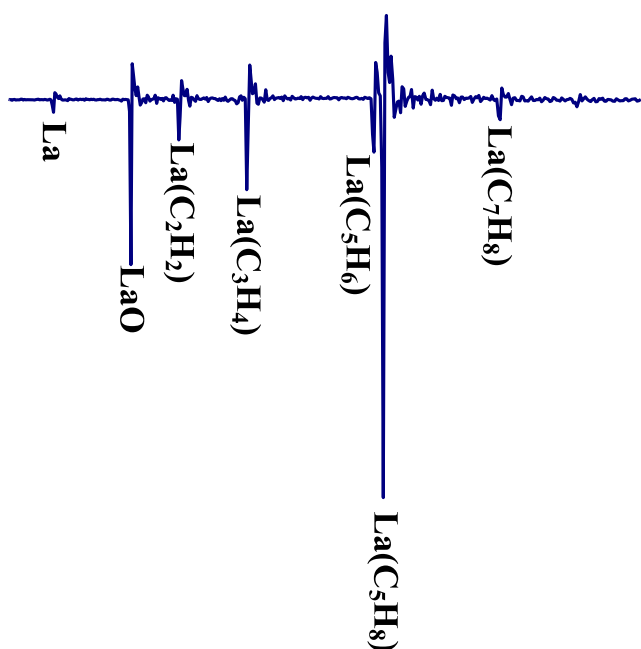

FIG. 1. TOF mass spectra of the La + isoprene reaction recorded with 235 nm laser ionization.
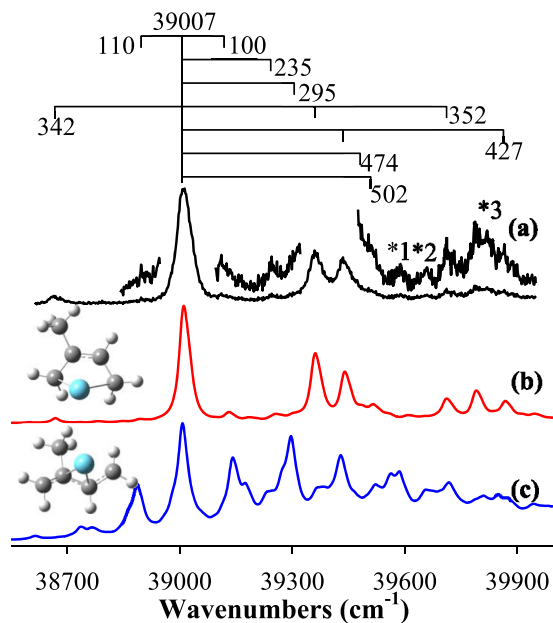
FIG. 2. MATI spectrum of La(C$_5$H$_8$) produced from the La + isoprene (a) and simulations of the ^{1}A ← ^{2}A transitions of Iso A (b) and Iso B (c) of La(C$_5$H$_8$) at 200 K. MATI bands labeled "*1-*3" are combinations bands.

for C1C2 and C3C4 but in an antibonding configuration for C2C3; on the other hand, the four C pπ orbitals of the lowest unoccupied molecular orbital (LUMO) are in an antibonding configuration for C1C2 and C3C4 but bonding for C2C3. Metal coordination depletes the diene pπ electron density of the HOMO due to donation of the pπ electrons to an empty La 5dσ orbital and populates the electron density of the LUMO by back electron donation from a filled La 5dπ orbital into the empty diene π^* orbital. The electron depletion in the HOMO and the electron population in the LUMO will thus have the
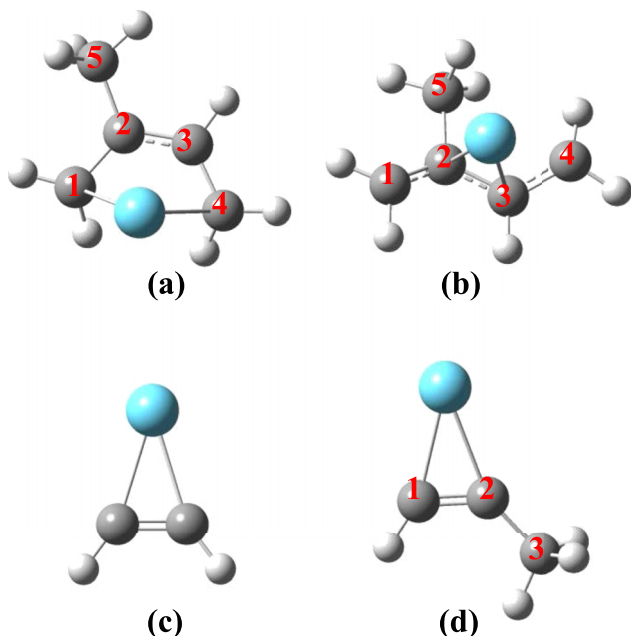
TABLE I. Molecular point groups, electronic states, and relative energies (cm^{-1}) of La(C$_5$H$_8$), La(C$_2$H$_2$), and La(C$_3$H$_4$) from the DFT/B3LYP and CCSD(T)//B3LYP calculations. The energies of La(C$_5$H$_8$) (Iso B) are relative to those of the La(C$_5$H$_8$) (Iso A) doublet ground state. All energies include vibrational zero-point energy corrections.

Complex	Point group	State	E$_{B3LYP}$	E$_{CCSD(T)}$
La(C$_5$H$_8$), Iso A	C$_1$	^{2}A	0	0
	C$_1$	^{1}A	39 600	38 692
La(C$_5$H$_8$), Iso B	C$_1$	^{2}A	3 559	2 823
	C$_1$	^{1}A	44 322	42 320
La(C$_2$H$_2$)	C$_{2v}$	^{2}A$_1$	0	0
	C$_{2v}$	^{1}A$_1$	42 107	40 889
La(C$_3$H$_4$)	C$_s$	^{2}A′	0	0
	C$_s$	^{1}A′	41 214	40 229

effect of lengthening the C1C2 and C3C4 distances and shortening the C2C3 bond length. Iso A is a five-membered ring obtained by rotating the C2C3 bond so that the isoprene carbon backbone is in a cis conformation. It has a significantly shorter C2C3 distance (1.388 Å) than C1C2 (1.451 Å) or C3C4 (1.455 Å) (Table S1 of the supplementary material). Because a five-membered ring is less strained than a three-membered one, Iso A is more stable than Iso B. In both Iso A and Iso B, the ground electronic state is a doublet with a La 6s^1-based valence electron configuration. The remaining two electrons that are associated with the isolated La atom are spin paired in a molecular orbital that is a bonding combination between the La 5dπ orbital and the diene π^* antibonding orbital. Removal of the La 6s electron by ionization yields a singlet ion.

The observed MATI spectrum is assigned to the ^{1}A ← ^{2}A transition of Iso A. This assignment is supported by the agreement between the measurement and computation (Table II and Fig. 2). Table II summarizes the measured and calculated AIEs and vibrational frequencies, and Fig. 2 compares the measured spectrum to the simulated vibronic spectrum of the ^{1}A ← ^{2}A transition of Iso A. The 0-0 transition in the simulation is aligned with the experimental origin band, but the computed vibrational frequencies are unscaled in order to directly compare with the measured spectrum. Based on the spectral simulation, the 352 and 427 cm^{-1} vibronic progressions are assigned to excitations of a La-ligand symmetric stretch coupled with a CH$_3$ rock (ν_{32}^+) and a La—C1/C4 symmetric stretch (ν_{30}^+) in the ^{1}A ion. The weak 100, 235, 295, 474, and 502 cm^{-1} vibronic bands are attributed to a CH$_3$ wag (ν_{36}^+), a C1—La—C4 bend (ν_{34}^+), a La—C1/C4 asymmetric stretch (ν_{33}^+), a CH$_2$ twist (ν_{29}^+) around C4, and another CH$_2$ twist (ν_{28}^+) around C1 in the ^{1}A ion as well. The hot bands at 110 and 342 cm^{-1} are due to thermal excitations of the CH$_3$ wag (ν_{36}) and La-ligand stretch (ν_{32}) in the ^{2}A neutral state. We have also considered a possible contribution from the ionization of Iso B, but it is excluded because the simulated transition is not consistent with the observed spectrum in both vibrational frequencies and spectral intensities [Fig. 2(c)].

FIG. 3. Structures of the ground states of Iso A (a) and Iso B (b) of La(C$_5$H$_8$), La(C$_2$H$_2$) (c), and La(C$_3$H$_4$) from the DFT/B3LYP calculations. Relative energies of these species are listed in Table I.

TABLE II. Adiabatic ionization energies (AIEs, cm^{-1}) and vibrational frequencies (cm^{-1}) of La(C$_5$H$_8$) (Iso A), La(C$_2$H$_2$), and La(C$_3$H$_4$) from MATI spectroscopy and DFT/B3LYP and CCSD(T)//B3LYP calculations. ν_n^+ and ν_n are the vibrational modes in the ionic and neutral states, and the energies in parentheses are from CCSD(T)//B3LYP calculations.

Complex	MATI	B3LYP [CCSD(T)]	Mode description[a]
La(C$_5$H$_8$) (Iso A), C$_1$, ^{1}A $\leftarrow$ ^{2}A			
AIE	39 007	39 600 (38 692)	
ν_{36}^+/ν_{36}	100/110	120/118	CH$_3$ wag
ν_{34}^+	235	246	C1—La—C4 bend
ν_{33}^+	295	291	La—C1/C4 asymmetric stretch
ν_{32}^+/ν_{32}	352/342	350/339	La-ligand stretch and CH$_3$ rock
ν_{30}^+	427	429	La—C1/C4 symmetric stretch
ν_{29}^+	474	478	CH$_2$ twist around C4
ν_{28}^+	502	506	CH$_2$ twist around C1
La(C$_2$H$_2$), C$_{2v}$, ^{1}A$_1$ $\leftarrow$ ^{2}A$_1$			
AIE	41 174	42 107 (40 889)	
ν_4^+/ν_4	522/495	528/498	La-ligand symmetric stretch
ν_3^+	806	832	In-plane C—H bend
La(C$_3$H$_4$), C$_s$, ^{1}A$'$ $\leftarrow$ ^{2}A$'$			
AIE	40 509	41 214 (40 229)	
ν_{12}^+	224	222	C2—CH$_3$ in-plane bend
ν_{11}^+	433	442	La—C2 stretch and C2—CH$_3$ in-plane bend
ν_{10}^+	572	570	La—C1 stretch and C1—H in-plane bend

[a]See Fig. 3 for the numbering of carbon atoms.

The formation of Iso A is exothermic without energy barriers as illustrated in Fig. 4. The figure presents the DFT/B3LYP computed stationary points, including reactants La + isoprene, intermediate state IM1, transition state TS1, and the product Iso A in their doublet spin states (except for isoprene which is in a singlet state). Energies of the stationary points
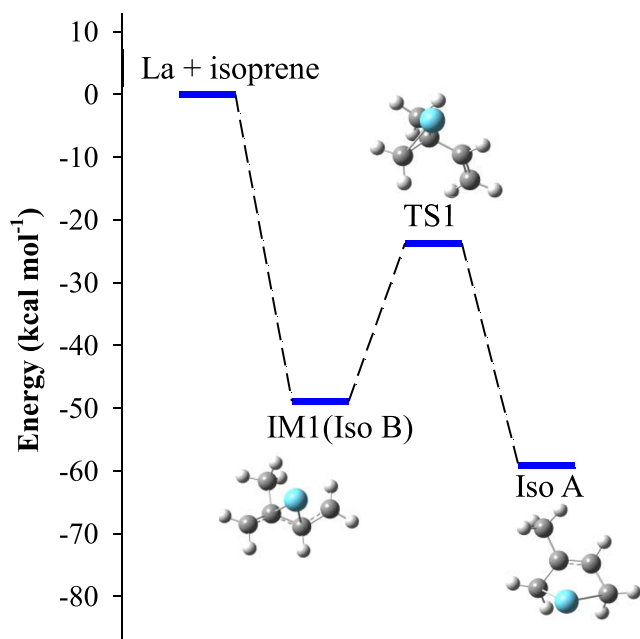

FIG. 4. Reaction pathway and energy profile for the formation of La(C$_5$H$_8$) (Iso A) from the La + isoprene reaction at the DFT/B3LYP level, where IM1 and TS1 stand for intermediate and transition states, respectively.

are reported in Table S2 of the supplementary material. IM1 is the same species as Iso B formed by La addition to the *trans*-isoprene and is located at 48.9 kcal mol^{-1} below the reactants in energy. Isomerization from IM1 to Iso A via TS1 shifts La bonding sites from the middle to terminal carbons and rotates the C2C3 bond to facilitate the formation of the five-membered metallacycle. The isomerization process is thermodynamically and kinetically favorable because Iso A is more stable than IM1, and TS1 is lower in energy than La + isoprene. Because of the low energy of TS1, IM1 has tendency to convert to Iso A even though it is predicted to be situated in the valley between the reactants and the transition state. This may explain why IM1 was not detected in our MATI measurements. Recently, we investigated La reactions with 1-butene, 2-butene, and isobutene under similar experimental conditions and found no association product but the dehydrogenated species as the major product in all three reactions.[48] The comparison of the isoprene and butene reactions under similar conditions suggests that the butadiene molecule is less reactive than the butenes. The lower reactivity of isoprene is largely due to the electron delocalization in the conjugated diene where all backbone carbons are in sp^2 hybridization.

C. La(C$_2$H$_2$)

Even though the number density of La(C$_2$H$_2$) was very low from the La + isoprene reaction (Fig. 5), we succeeded in obtaining a sharp MATI spectrum for this species [Fig. 5(a)]. The spectrum exhibits a strong origin band at 41 174 (5) cm^{-1},
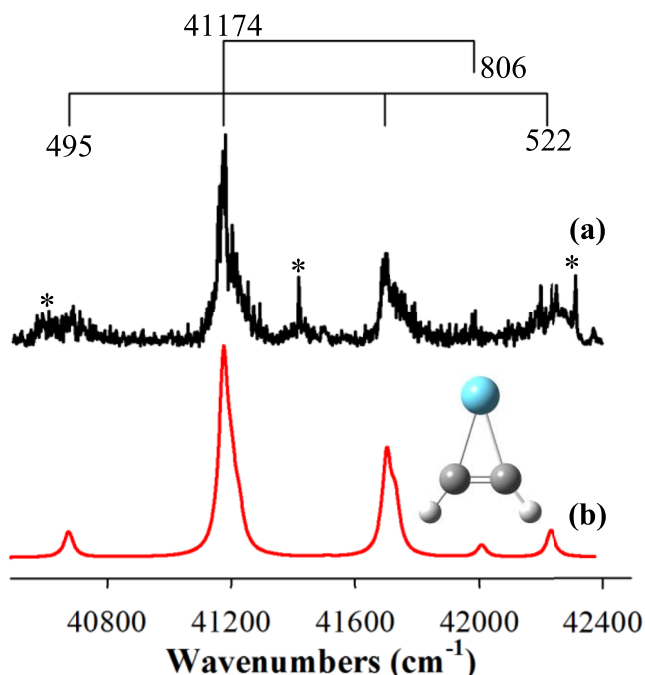
FIG. 5. MATI spectrum of La(C$_2$H$_2$) produced from the La + isoprene (a) and simulation of the $^1A_1 \leftarrow {}^2A_2$ transition of La(C$_2$H$_2$) at 500 K (b). Sharp lines marked with "*" are due to the interference from LaO.

a 522 cm^{-1} vibronic progression with up to two quanta and a weak vibronic band at 806 cm^{-1} to the blue of the origin band, and a hot band at 495 cm^{-1} to red of the origin band. The origin band and vibronic transition energies are the same as those observed for La(C$_2$H$_2$) produced in La reactions with ethylene and 1,3-butadiene,[42,44] though the signal to noise ratios are not as good due to a much lower number density of the species formed in this reaction. The spectrum can easily be assigned to the $^1A_1 \leftarrow {}^2A_1$ transition of lanthanacyclopropene [C$_{2v}$, Fig. 3(c)] by comparing with the spectra of La(C$_2$H$_2$) from the ethylene and 1,3-butadiene reactions and with the simulated spectrum in Fig. 5(b). The transition energy of the origin band, 41 174 cm^{-1}, corresponds to the AIE of the species. The 522 cm^{-1} progression is due to excitations of the La—C$_2$H$_2$ symmetric stretch (ν_4^+) and the 806 cm^{-1} vibronic band to the in-plane C—H bend (ν_3^+) in the $^1A_1$ ion, and the 459 cm^{-1} hot band is assigned to the thermal excitation of the metal-ligand stretch in the $^2A_1$ neutral species (Table II). It is noted that the spectrum of La(C$_2$H$_2$) is vibrationally much hotter than that of La(C$_5$H$_8$) because a temperature of ~500 K is required to simulate the 495 cm^{-1} hot band of the La(C$_2$H$_2$) spectrum [Fig. 5(b)], whereas a temperature of ~200 K is sufficient for simulating the 110 and 342 cm^{-1} hot bands of the La(C$_5$H$_8$) Iso A spectrum [Fig. 2(b)]. Different vibrational temperatures for molecules of various sizes seeded in molecular beams are not unusual because the internal modes of the molecules are typically not at thermal equilibria. Generally, smaller molecules with higher vibrational-frequency modes have higher vibrational temperatures than larger molecules with softer vibrational modes. It is also noted that the vibrational temperature of La(C$_2$H$_2$) formed in the La + isoprene reaction is considerably higher (~500 K) than that of La(C$_2$H$_2$) from the La + ethylene reaction (~300 K).[42] This is because La(C$_2$H$_2$) formed by the

C—C bond cleavage of isoprene is strongly exothermic (by 20.6 kcal mol^{-1}) as discussed below, whereas La(C$_2$H$_2$) formed through the dehydrogenation of ethylene is only weakly exothermic (by 4.7 kcal mol^{-1}). A reaction with higher exothermicity is expected to deposit more energy in the internal modes of resultant products than a reaction with lower exothermicity.

A plausible reaction pathway for the formation of La(C$_2$H$_2$) from the La + isoprene reaction is illustrated in Fig. 6. It includes La association and insertion, H migration, and C—C bond cleavage. La addition to form association species Iso A has been discussed in a previous paragraph. The second step is La insertion into a C—H bond of the CH$_2$ group in the C4 position to form inserted species IM2. Following the La—H rotation through TS3, the La-bonded H is migrated to C3 and a new lanthanacyclopentene, IM3, is formed with La bonding to both terminal carbon atoms. Although IM3 and Iso A are both five-membered metallacycles, their structures are considerably different, and IM3 is significantly less stable. In IM3, the carbon backbone is non-planar with C3C4 being a double bond, C1C2 and C2C3 being single bonds, and the five-membered ring in a boat-like conformation. On the other hand, the carbon backbone in Iso A is planar with CC distances longer than a C=C double bond but shorter than a C—C single bond (1.388–1.455 Å) and the five-membered ring in a chair-like shape. Like an organic cyclic molecule, the boat-like conformer IM3 is less stable than the chair-like conformer Iso A. Additionally, the delocalized CC bonds are expected to contribute to the stability of Iso A. The last step is the C2C3 bond cleavage to form La(C$_2$H$_2$) + propene. The cracking of the C2C3 bond is facilitated via TS4, where one of the La binding sites shifts from C1 to C3 and the C1C2 bond becomes a double bond. The whole process is exothermic by 20.6 kcal mol^{-1} and has no barriers above the reactant energies.
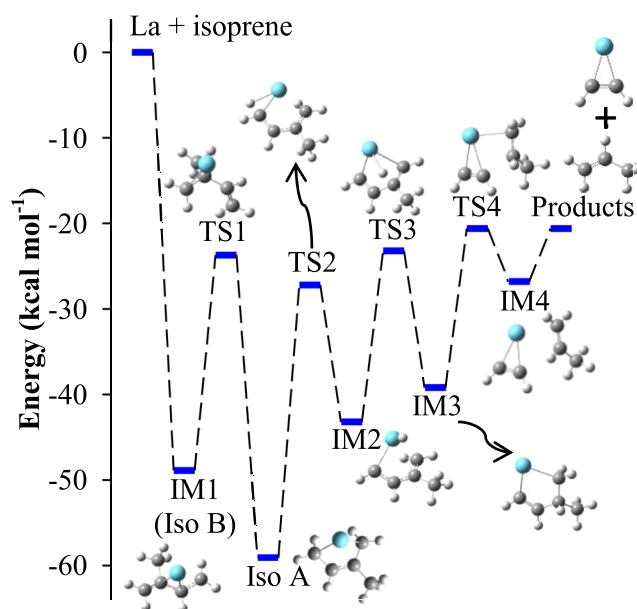

FIG. 6. Reaction pathway and energy profile for the formation of La(C$_2$H$_2$) from the La + isoprene reaction at the DFT/B3LYP level, where IMn stands for intermediates and TSn stands for transition states.

D. La(C$_3$H$_4$)

The MATI spectrum of La(C$_3$H$_4$) [Fig. 7(a)] exhibits a strong origin band at 40 509 (5) cm^{-1} and weak bands at 224, 433, and 572 cm^{-1} above the origin band. The spectrum resembles one of the two band systems observed for La(C$_3$H$_4$) formed through La-mediated dehydrogenation of propene.[45] In the previous study of the La + propene reaction, four isomers of La(C$_3$H$_4$) were considered, two of which, La(CHCCH$_3$) (C$_s$) and La(CHCHCH$_2$) (C$_1$), were detected with MATI spectroscopy. By comparing with the MATI spectrum of La(C$_3$H$_4$) formed in the La + propene reaction and with the simulated spectrum in Fig. 7(b), the experimental spectrum in Fig. 7(a) is assigned to the ^{1}A$'$ ← ^{2}A$'$ transition of La(CHCCH$_3$) [C$_s$, Fig. 3(d)]. The 224, 433, and 572 cm^{-1} vibronic bands are attributed to excitations of a C2—CH$_3$ in-plane bend (ν_{12}^+), a La—C2 stretch coupled with a C2—CH$_3$ in-plane bend (ν_{11}^+), and a La—C1 stretch coupled with C1—H in-plane bend (ν_{10}^+) of the ^{1}A$'$ ion. The calculated frequencies for the ν_{12}^+, ν_{11}^+, and ν_{10}^+ modes are 222, 442, and 570 cm^{-1} which are in excellent agreement with the measured values (Table II).

The reaction pathway for the formation of La(CHCCH$_3$) is similar to that of La(C$_2$H$_2$), which involves La addition and insertion, H migration, and C—C bond cleavage as illustrated in Fig. 8. However, the C—H bond that is activated by La insertion and the carbon atom to which the H atom migrates are different between the pathways for the formation of the two species. In the formation of La(C$_2$H$_2$) (Fig. 6), La inserts into a C4—H bond (IM2) and the La-bonded H migrates to C2 (IM3); on the other hand, in the formation of La(CHCCH$_3$) (Fig. 8), La insertion occurs at a C1—H bond (IM5) and the H migration occurs at C3 (IM6). Nevertheless, because C4—H and C1—H bonds are very similar, energies required for La insertion into the two C—H bonds (TS2 and TS5) are almost
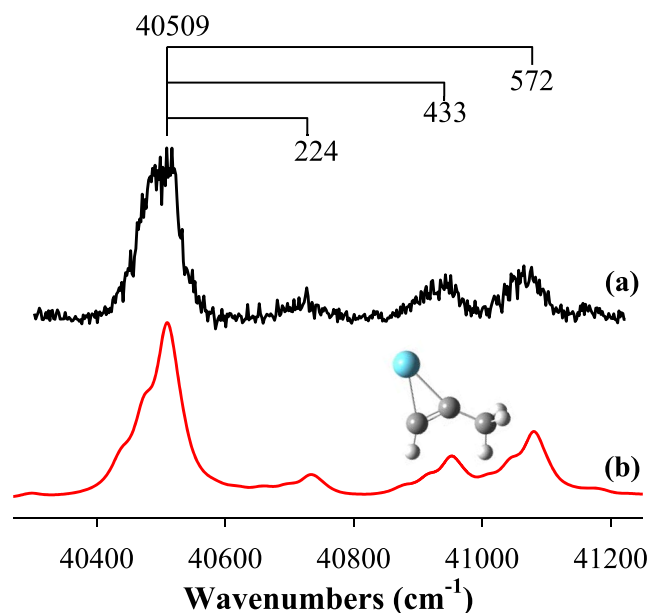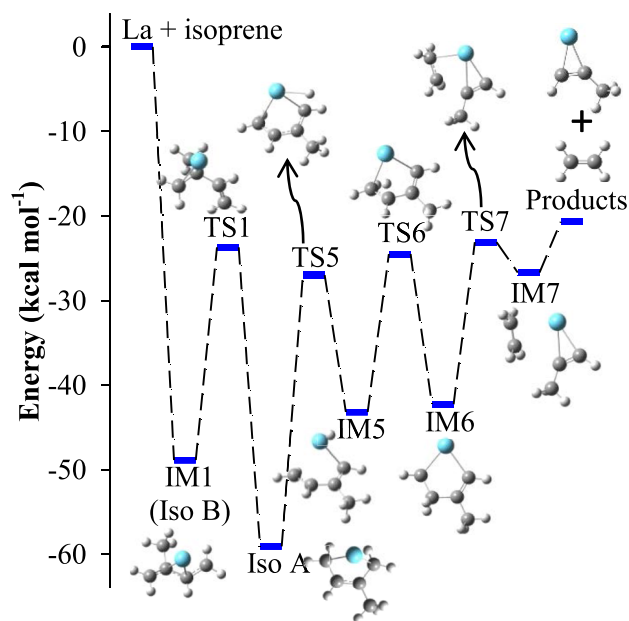

FIG. 8. Reaction pathway and energy profile for the formation of La(C$_3$H$_4$) from the La + isoprene reaction at the DFT/B3LYP level, where IMn stands for intermediates and TSn stands for transition states.

identical and so are the energies of the resultant inserted species (IM2 and IM5) (Table S2 of the supplementary material). Likewise, the barriers for the La-bonded H migrations (TS3 and TS6) are close and so are the resultant five-membered lanthanacycles (IM3 and IM6). The main difference between IM3 and IM6 is the location of the C=C double bonds which are C3=C4 in IM3 and C1=C2 in IM6. The cleaved C—C bonds in the formation of both La(C$_2$H$_2$) and La(CHCCH$_3$) are the same C2—C3 bond. The different products from cracking the same bond are due to the methyl substitution of a H atom in 1,3-butadiene which yields an asymmetric butadiene with respect to the center point of the C2—C3 single bond.

IV. CONCLUSIONS

We have reported the MATI spectra and formation of La(C$_5$H$_8$), La(C$_2$H$_2$), and La(C$_3$H$_4$) formed through La addition and C—C bond cleavage of isoprene. The spectra of all three species display a single band system consisting of a strong origin band and several weak vibronic bands. The MATI measurements yield the AIEs and metal-ligand stretching and ligand-based bending frequencies for the three species. Comparing the spectroscopic measurements with quantum chemical calculations allows for the identification of the structures and electronic states of these species. La(C$_5$H$_8$) is a five-membered metallacycle, whereas La(C$_2$H$_2$) and La(C$_3$H$_4$) are both three-membered rings. The ground state of each species is a doublet state with a La based 6s^1 electron configuration, and the lowest-energy state of the corresponding ion is a singlet state upon the removal of the La 6s^1 electron. Because of the largely non-bonding nature of the La 6s^1 electron, ionization has a small effect on the geometry of the neutral state of each species. Computational reaction pathways show that the formation of La(C$_5$H$_8$) involves La addition and isoprene isomerization; the formation of La(C$_2$H$_2$) and La(C$_3$H$_4$) each

FIG. 7. MATI spectrum of La(C$_3$H$_4$) produced from the La + isoprene reaction (a) and simulation of the ^{1}A$'$ ← ^{2}A$'$ transition of La(C$_3$H$_4$) at 300 K (b).

consists of La addition, La insertion into a C—H bond, H migration, and C—C bond cleavage; the formation of the all three species are thermodynamically and kinetically favorable. The observation of both $La(C_2H_2)$ and $La(C_3H_4)$ confirms that the carbon-carbon bond cracking occurs at the C2—C3 bond of isoprene.

SUPPLEMENTARY MATERIAL

See supplementary material for the geometries of $La(C_5H_8)$ and its singly charged positive ion and the energies of the stationary points along the reaction coordinates for the formation of $La(C_5H_8)$ (Iso A), $La(C_2H_2)$, and $La(C_3H_4)$ from the La atom reaction with isoprene.

ACKNOWLEDGMENTS

[1] R. S. Walters, T. D. Jaeger, and M. A. Duncan, J. Phys. Chem. A **106**, 10482 (2002).

[2] R. S. Walters, E. D. Pillai, P. v. R. Schleyer, and M. A. Duncan, J. Am. Chem. Soc. **127**, 17030 (2005).

[3] R. S. Walters, P. V. Schleyer, C. Corminboeuf, and M. A. Duncan, J. Am. Chem. Soc. **127**, 1100 (2005).

[4] A. D. Brathwaite, T. B. Ward, R. S. Walters, and M. A. Duncan, J. Phys. Chem. A **119**, 5658 (2015).

[5] R. B. Metz, Adv. Chem. Phys. **138**, 331 (2008).

[6] G. Altinay, M. Citir, and R. B. Metz, J. Phys. Chem. A **114**, 5104 (2010).

[7] G. Altinay and R. B. Metz, J. Am. Soc. Mass Spectrom. **21**, 750 (2010).

[8] G. Altinay and R. B. Metz, Int. J. Mass Spectrom. **297**, 41 (2010).

[9] M. Citir, G. Altinay, G. Austein-Miller, and R. B. Metz, J. Phys. Chem. A **114**, 11322 (2010).

[10] G. Altinay, A. Kocak, J. S. Daluz, and R. B. Metz, J. Chem. Phys. **135**, 084311 (2011).

[11] M. Perera, P. Ganssle, and R. B. Metz, Phys. Chem. Chem. Phys. **13**, 18347 (2011).

[12] A. Kocak, M. A. Ashraf, and R. B. Metz, J. Phys. Chem. A **119**, 9653 (2015).

[13] A. Kocak, Z. Sallese, M. D. Johnston, and R. B. Metz, J. Phys. Chem. A **118**, 3253 (2014).

[14] M. A. Ashraf, C. W. Copeland, A. Kocak, A. R. McEnroe, and R. B. Metz, Phys. Chem. Chem. Phys. **17**, 25700 (2015).

[15] C. W. Copeland, M. A. Ashraf, E. M. Boyle, and R. B. Metz, J. Phys. Chem. A **121**, 2132 (2017).

[16] V. J. F. Lapoutre, B. Redlich, A. F. G. van der Meer, J. Oomens, J. M. Bakker, A. Sweeney, A. Mookherjee, and P. B. Armentrout, J. Phys. Chem. A **117**, 4115 (2013).

[17] O. W. Wheeler, M. Salem, A. Gao, J. M. Bakker, and P. B. Armentrout, J. Phys. Chem. A **120**, 6216 (2016).

[18] S. R. Miller, T. P. Marcy, E. L. Millam, and D. G. Leopold, J. Am. Chem. Soc. **129**, 3482 (2007).

[19] W. Y. Lu, P. D. Kleiber, M. A. Young, and K. H. Yang, J. Chem. Phys. **115**, 5823 (2001).

[20] A. S. Gentlman, A. E. Green, D. R. Price, E. M. Cunningham, A. Iskra, and S. R. Mackenzie, Top. Catal. **61**, 81 (2018).

[21] G. C. Boles, R. A. Coates, G. Berden, J. Oomens, and P. B. Armentrout, J. Phys. Chem. B **120**, 12486 (2016).

[22] G. C. Boles, R. A. Coates, G. Berden, J. Oomens, and P. B. Armentrout, J. Phys. Chem. B **119**, 11607 (2015).

[23] G. C. Boles, C. J. Owen, G. Berden, J. Oomens, and P. B. Armentrout, Phys. Chem. Chem. Phys. **19**, 12394 (2017).

[24] R. A. Coates, G. C. Boles, C. P. McNary, G. Berden, J. Oomens, and P. B. Armentrout, Phys. Chem. Chem. Phys. **18**, 22434 (2016).

[25] R. A. Coates, C. P. McNary, G. C. Boles, G. Berden, J. Oomens, and P. B. Armentrout, Phys. Chem. Chem. Phys. **17**, 25799 (2015).

[26] J. A. Maner, D. T. Mauney, and M. A. Duncan, J. Phys. Chem. Lett. **6**, 4493 (2015).

[27] G. X. Liu, S. M. Ciborowski, and K. H. Bowen, J. Phys. Chem. A **121**, 5817 (2017).

[28] R. B. Wyrwas, B. L. Yoder, J. T. Maze, and C. C. Jarrold, J. Phys. Chem. A **110**, 2157 (2006).

[29] S. Xu, J. E. T. Smith, and J. M. Weber, Inorg. Chem. **55**, 11937 (2016).

[30] S. Xu, J. E. T. Smith, and J. M. Weber, J. Phys. Chem. A **120**, 7650 (2016).

[31] S. Xu, J. E. T. Smith, and J. M. Weber, J. Chem. Phys. **145**, 024304 (2016).

[32] S. Xu, J. E. T. Smith, and J. M. Weber, J. Phys. Chem. A **120**, 2350 (2016).

[33] J. W. DePalma, P. J. Kelleher, L. C. Tavares, and M. A. Johnson, J. Phys. Chem. Lett. **8**, 484 (2017).

[34] M. U. Munshi, S. M. Craig, G. Berden, J. Martens, A. F. DeBlase, D. J. Foreman, S. A. McLuckey, J. Oomens, and M. A. Johnson, J. Phys. Chem. Lett. **8**, 5047 (2017).

[35] D. J. Brugh, R. S. Dabell, and M. D. Morse, J. Chem. Phys. **121**, 12379 (2004).

[36] M. A. Garcia and M. D. Morse, J. Phys. Chem. A **117**, 9860 (2013).

[37] D. J. Brugh and M. D. Morse, J. Chem. Phys. **141**, 064304 (2014).

[38] E. L. Johnson and M. D. Morse, Mol. Phys. **113**, 2255 (2015).

[39] M. A. Flory, A. J. Apponi, L. N. Zack, and L. M. Ziurys, J. Am. Chem. Soc. **132**, 17186 (2010).

[40] D. Hewage, M. Roudjane, W. R. Silva, S. Kumari, and D.-S. Yang, J. Phys. Chem. A **119**, 2857 (2015).

[41] D. Hewage, W. R. Silva, W. Cao, and D.-S. Yang, J. Am. Chem. Soc. **138**, 2468 (2016).

[42] S. Kumari, W. Cao, Y. Zhang, M. Roudjane, and D.-S. Yang, J. Phys. Chem. A **120**, 4482 (2016).

[43] Y. Zhang, M. W. Schmidt, S. Kumari, M. S. Gordon, and D.-S. Yang, J. Phys. Chem. A **120**, 6963 (2016).

[44] D. Hewage, W. Cao, J. H. Kim, Y. Wang, Y. Liu, and D.-S. Yang, J. Phys. Chem. A **121**, 1233 (2017).

[45] S. Kumari, W. Cao, D. Hewage, R. Silva, and D.-S. Yang, J. Chem. Phys. **146**, 074305 (2017).

[46] D. Hewage, W. Cao, S. Kumari, R. Silva, T. H. Li, and D.-S. Yang, J. Chem. Phys. **146**, 184304 (2017).

[47] W. Cao, D. Hewage, and D.-S. Yang, J. Chem. Phys. **147**, 064303 (2017).

[48] W. Cao, D. Hewage, and D.-S. Yang, J. Chem. Phys. **148**, 044312 (2018).

[49] J. Huang, Z. Liu, D. Cui, and X. Liu, ChemCatChem **10**, 42 (2018).

[50] V. Baranov, H. Becker, and D. K. Bohme, J. Phys. Chem. A **101**, 5137 (1997).

[51] P. I. Surya, D. R. A. Ranatunga, and B. S. Freiser, J. Am. Chem. Soc. **119**, 3351 (1997).

[52] P. Mourgues, A. Ferhati, T. B. McMahon, and G. Ohanessian, Organometallics **16**, 210 (1997).

[53] K. A. Zemski, R. C. Bell, and A. W. Castleman, Int. J. Mass. Spetrom. **184**, 119 (1999).

[54] K. A. Zemski, R. C. Bell, and A. W. Castleman, Jr., J. Phys. Chem. A **104**, 5732 (2000).

[55] R. C. Bell, K. A. Zemski, K. P. Kerns, H. T. Deng, and A. W. Castleman, J. Phys. Chem. A **102**, 1733 (1998).

[56] F. Dong, S. Heinbuch, Y. Xie, E. R. Bernstein, J. J. Rocca, Z.-C. Wang, X.-L. Ding, and S.-G. He, J. Am. Chem. Soc. **131**, 1057 (2009).

[57] B. R. Sohnlein, S. G. Li, J. F. Fuller, and D.-S. Yang, J. Chem. Phys. **123**, 014318 (2005).

[58] C. E. Moore, *Atomic Energy Levels* (National Bureau of Standards, Washington, DC, 1971).

[59] M. A. Duncan, T. G. Dietz, and R. E. Smalley, J. Chem. Phys. **75**, 2118 (1981).

[60] D.-S. Yang, J. Phys. Chem. Lett. **2**, 25 (2011).

[61] T. H. Dunning, Jr., J. Chem. Phys. **90**, 1007 (1989).

[62] W. A. de Jong, R. J. Harrison, and D. A. Dixon, J. Chem. Phys. **114**, 48 (2001).

[63] Q. Lu and K. A. Peterson, J. Chem. Phys. **145**, 054111 (2016).

[64] M. J. Frish, G. W. Trucks, H. B. Schlegel, G. E. Scuseria, M. A. Robb, J. R. Cheeseman, G. Scalmani, V. Barone, B. Mennucci, G. A. Petersson, H. Nakatsuji, M. Caricato, X. Li, H. P. Hratchian, A. F. Izmaylov, J. Bloino, and G. Zheng, GAUSSIAN 09, Revision A.01, Gaussian, Inc., Wallingford, CT, 2009.

[65] H.-J. Werner, P. J. Knowles, G. Knizia, F. R. Manby, M. Schutz, P. Celani, T. Korona, R. Lindh, A. Mitrushenkov, G. Rauhut, K. R. Shamasundar, T. B. Adler, R. D. Amos, A. Bernhardsson, A. Berning, D. L. Cooper, M. J. O. Deegan, A. J. Dobbyn, F. Eckert, E. Goll, C. Hampel, A. Hesselmann, G. Hetzer, T. Hre-nar, G. Jansen, C. Koppl, Y. Liu, A. W. Lloyd,

R. A. Mata, A. J. May, S. J. McNicholas, W. Meyer, M. E. Mura, A. Nicklass, D. P. O'Neill, P. Palmieri, K. Pfluger, R. Pitzer, M. Reiher, T. Shiozaki, H. Stoll, A. J. Stone, R. Tarroni, T. Thorsteinsson, M. Wang, and A. Wolf, MOLPRO, version 2010.1, a package of *ab initio* programs, 2010, see http://www.molpro.net.

[66] S. Li, "Threshold photoionization and ZEKE photoelectron spectroscopy of metal complexes," Ph.D. thesis, University of Kentucky, 2004.
[67] E. V. Doktorov, I. A. Malkin, and V. I. Man'ko, J. Mol. Spectrosc. **64**, 302 (1977).
[68] F. Duschinsky, Acta Physicochim. **7**, 551 (1937).